Acta Biochim Biophys Sin 2010, 42: 472–482 | © The Author 2010. Published by ABBS Editorial Office in association with Oxford University Press on behalf of the Institute of Biochemistry and Cell Biology, Shanghai Institutes for Biological Sciences, Chinese Academy of Sciences. DOI: 10.1093/abbs/gmq047.

Original Article

Connexin 43 hemichannel regulates H9c2 cell proliferation by modulating intracellular ATP and [Ca^{2+}]

Dongli Song†, Xiaoyu Liu†, Rujiao Liu, Ling Yang, Ji Zuo*, and Wen Liu*

Department of Cellular and Genetic Medicine, Shanghai Medical College, Fudan University, Shanghai 200032, China
†These authors contributed equally to this work.
*Correspondence address. Tel/Fax: +86-21-54237311; E-mail: jzuo@shmu.edu.cn (J.Z.)/liuwen@shmu.edu.cn (W.L.)

Connexin 43 (Cx43), known to be the main protein building blocks of gap junctions and hemichannels in mammalian heart, plays an important role in cardiocytes proliferation. Gap junctional intercellular communication has been suggested to be necessary for cellular proliferation and differentiation. However, the effect of Cx43 hemichannel on cardiocytes proliferation and the mechanism remain unclear. In this study, rat heart cell line H9c2 was used. The Cx43 location, the proliferation rate and hemichannel activity of H9c2 cells and Wnt-3a^{+}-H9c2 cells were investigated and the changes of intracellular ATP and [Ca^{2+}] were determined. Results showed that the inhibited hemichannel induced by 18β-glycyrrhetinic acid (GA) evoked intracellular ATP and [Ca^{2+}] increase and enhanced H9c2 cell proliferation. Wnt-3a^{+}-H9c2 cells displayed enhanced hemichannel activity and proliferation rate. Inhibited hemichannel of Wnt-3a^{+}-H9c2 cells induced by 18β-GA decreased intracellular ATP, increased [Ca^{2+}], and enhanced the proliferation of H9c2 cells. This study validated the role of hemichannel in H9c2 cell proliferation regulation, and showed a mechanism involved in the regulation of H9c2 cell proliferation. The proliferation could be enhanced by Cx43 hemichannel-mediated ATP release accompanying intracellular [Ca^{2+}] change. However, different changes of ATP were observed in Wnt-3a^{+}-H9c2 cells. These findings provided new insights into the molecular mechanisms of proliferation regulation in H9c2 cells and the effect of Wnt-3a on intracellular ATP.

Keywords Wnt-3a; connexin 43; H9c2 cell; hemichannel; proliferation

Received: March 6, 2010 Accepted: May 5, 2010

Introduction

Connexins are a family of proteins that allow the synthesis of a large number of different connexons and gap junction (GJ) channels, which consist of 20 connexin isoforms in the mouse genome and 21 in the human genome [1]. Each connexin contains four transmembrane domains connected by two extracellular segments flanked by intracellular amino and carboxy terminal ends [1,2]. Functional GJ channels are formed by two docking and opening hemichannels, contributed by each of the adjoining cells. Each hemichannel or connexon is composed of six compatible connexin subunits; they are assembled in the intracellular compartment and transported to the plasma membrane [3–5]. The major GJ protein of mammalian cardiomyocytes is connexin 43 (Cx43). GJs form transmembrane channels that mediate direct cell–cell communication, which allow the passage of molecules and ions <1 kDa [6], including small metabolites, and second messengers such as sodium, potassium, calcium, cAMP/cGMP, and ADP/ATP to translocate from cell to cell [7,8].

Recently, Cx43 hemichannels have been observed to play a role in several physiological and pathological processes including volume regulation [9], efflux of NAD^{+} and ATP [10–12]. It is likely that hemichannels serve as one pathway for the release of these small substances present intracellularly [5]. In order to study the function of hemichannel, it is necessary to find a substance that selectively blocks this type of channel without affecting GJ. However, all of GJ blockers have also been used to inhibit hemichannel-mediated currents under physiological conditions. Glycyrrhetinic acid (GA), an aglycone saponin extracted from licorice root, which is known to be essential for its anti-inflammatory and anti-ulcerous activities, has been widely used as a potent inhibitor of gap junctional intercellular communication (GJIC) and hemichannel activity [13,14]. The mechanism involved in the inhibition of 18β-GA is Src-mediated phosphorylation of Cx43 [15]. Wnt signaling is an important modulator of Cx43, and local accumulation of Cx43 transcript expression was observed in the limb mesenchyme of transgenic mice ectopically expressing Wnt-1 [16]. Our previous report also

confirmed that the expression of Cx43 in Wnt-3a$^+$-H9c2 cells was increased and the proliferation rate of Wnt-3a$^+$-H9c2 cells was changed [17].

Intracellular ATP has emerged as energy source and phosphate donor in enzymatic processes and extracellular ATP may activate specific membrane receptors, the P2 purinergic receptor family, to be involved in various cell processes such as regulation of cardiovascular functions [18]. ATP is found to be essential in the generation of neuron during embryonic development. Sanches *et al*. [19] have shown that ATP increases DNA synthesis in retinal cultures prepared from chicken embryos with no more than 7 or 8 days *in vivo*. The retinal pigment epithelium (RPE) releases ATP by efflux through Cx43 hemichannels to control the proliferation of neuronal precursor cells [20]. Ca^{2+} signaling induced by cADPR generated from NAD^+ released through Cx43 hemichannels increase the proliferation rate of 3T3 fibroblasts via shorten its S phase [21]. ATP, which has been known as the diffusible messenger in cell signaling pathways in many cell types, is characterized to induce elevation of intracellular astrocytic $[Ca^{2+}]i$ [21].

GJIC has been widely considered to be involved in cardiocytes proliferation and differentiation. However, the effect of Cx43 hemichannel on proliferation of H9c2 cells and the mechanism remain unclear. As our previous report confirmed that the expression of Cx43 in Wnt-3a$^+$-H9c2 cells was increased [17], we further examined the proliferation rate and the Cx43 transcription and intracellular location in H9c2 and Wnt-3a$^+$-H9c2 cells. The activity of hemichannel in Wnt-3a$^+$-H9c2 cells was measured by EthBr uptake and the fluorescence was found to be increased. So we used Wnt-3a transfected cells to increase hemichannel activity and 18β-GA to block hemichannels and studied their effects on cell proliferation. Then the intracellular $[Ca^{2+}]$ and ATP changes were examined in H9c2 and Wnt-3a$^+$-H9c2 cells treated with 18β-GA. We found that the intracellular ATP released and $[Ca^{2+}]$ changes were the signals by which the hemichannel regulated proliferation of H9c2 cells, but they were not modulated in parallel.

Materials and Methods

Materials

H9c2 was purchased from American Type Culture Collection (ATCC, Manassas, USA). 18β-GA, EthBr, and Furosemide were purchased from Sigma (St. Louis, USA). Carboxy-dichloro-fluorescein (CDCF), Lipofectamine 2000, fluo-3 AM, and Trizol reagent were purchased from Invitrogen (Grand Island, USA). RevertAid first strand cDNA synthesis kit and reverse transcription (RT) system were purchased from MBI Fermentas Inc. (Amherst, USA). Mouse Myc antibody and chemiluminescence kit was purchased from Beyotime (Hangzhou, China). Peroxidase-conjugated donkey anti-rabbit IgG antibody and peroxidase-conjugated rabbit anti-mouse IgG antibody was obtained from Santa Cruz Biotechnology (Santa Cruz, USA). The 3-(4, 5-dimethyl-2-thiazol-yl)-2, 5-diphenyl-2H-tetrazolium bromide (MTT) was purchased from Amresco (Solon, USA). FITC-labeled goat anti-rabbit antibody was purchased from Jackson ImmunoResearch Laboratories, Inc. (West Grove, USA). Bicinchoninic acid protein assay kit was obtained from Biocolors (Shanghai, China). The designed primers were synthesized by Shanghai Sangon Biological Engineering Technology & Services Co. (Shanghai, China).

X-ray film was purchased from Eastman Kodak (Rochester, USA). Glass coverslips were obtained from Shengyou Biotechnology Co., Ltd (Hangzhou, China). Centrifugal filter devices were purchased from Millipore (Billerica, USA).

Cell culture and transfections

H9c2 cells were grown in Dulbecco's modified Eagle's medium supplemented with 10% fetal bovine serum. Cells were transfected with *Wnt-3a* by Lipofectamine 2000 as recommended by the manufacturer. For stable transfection, cells were cultured in selection medium containing 0.8% G418, and cells clones were selected as described previously. The stably transfected cells were maintained in cell culture medium containing 0.5% G418 [22].

Real-time polymerase chain reaction

Total RNA was isolated from H9c2 and Wnt-3a$^+$-H9c2 cells with or without the treatment of 18β-GA using Trizol reagent. The first stranded complementary DNA was synthesized from 2 μg of total RNA using revert aid first strand cDNA synthesis kit. RT was carried out at 42°C for 30 min followed by incubation at 95°C for 5 min. cDNA amplification was carried out under the temperature profile: 94°C for 30 s; 55°C for 30 s; and 72°C for 1 min. At the end of 35 cycles, the reaction was prolonged for 10 min at 72°C, and then 5 μl of product was analyzed on 1.5% agarose gel. The following are the sequences of the primers: *Cx43* sense, 5′-TTGTTTCTGTCACCAGTAA C-3′; *Cx43* antisense, 5′-GATGAGGAAGGAAGAGAA GC-3′; *β-actin* sense, 5′-AGGCATCCTGACCCTGAAG TAC-3′; *β-actin* antisense, 5′-GAGGCATACAGGGACAA CACAG-3′ [17]. The samples were separated on 1.8% EthBr-stained agarose gel. As an internal control, *β-actin* was detected and as a negative control [23]. Results were analyzed by Quantity One.

Western blot analysis

The supernatants of culture media were filtrated and the samples were centrifuged at 7500 *g* for 10 min at 4°C. The proteins were obtained using the centrifugal filter devices.

Theses supernatants were denatured by heating at 95°C for 5 min in protein sample buffer (295 mM sucrose, 2% SDS,

2.5 mM EDTA, 62.5 mM Tris–HCl, pH 8.8, 0.05% bromophenol blue, and 26 mM dithiothreitol). Protein concentrations were determined using a Bicinchoninic acid protein assay kit. A total of 30 μg protein of cellular lysates was then electrophoresed on 10% SDS-polyacrylamide gel and transferred to polyvinylidene difluoride membranes by electroblotting. The membranes were incubated in 5% nonfat milk overnight, then incubated with mouse anti-Myc antibody (1:500) for 2 h at room temperature, followed by incubation with peroxidase-conjugated anti-rat IgG (1:5000) or anti-mouse IgG (1:5000) for 1 h at room temperature. Immunoreactive proteins were visualized using a commercially available enhanced chemiluminescence kit with exposure of the transfer membrane to X-ray film [24].

Measurement of hemichannel permeability: dye uptake

For visualization of dye uptake by captured images, cells were exposed to 0.5 μM EthBr for 10 min at 37°C. Then, cells were washed with HBSS (137 mM NaCl, 5.4 mM KCl, 0.34 mM Na_2HPO_4, and 0.44 mM KH_2PO_4, pH 7.4) supplemented with 1.2 mM $CaCl_2$ (HBSS-Ca^{2+}). For EthBr uptake, H9c2 cells were mounted in Fluoromount and examined by epifluorescence (518 nm excitation and 605 nm emission) using an inverted microscope (Diaphot-Nikon, Toyota, Japan) equipped with a CCD camera (Nikon, Toyota, Japan) associated with image analyzer software (Lucia-Nikon, Toyota, Japan). Captured images of EthBr uptake were analyzed with the NIH ImageJ program [25].

Measurement of gap junctional permeability: fluorescence recovery after photobleaching

This technique was used to assess gap junctional intracellular communication. Briefly, H9c2 cells were seeded on 20-mm glass coverslips in the bottom of 35 mm^2 plates at the density of 5×10^3 cells/cm^2 or 5×10^4 cells/$cm^2$and grown for 24–36 h [26]. In the fluorescence recovery after photobleach procedure (FRAP), the cultures were loaded with CDCF diacetate for 5 min, washed for three times, and incubated at room temperature for an additional 20 min. A baseline fluorescence image of the culture was first obtained, and the area of laser scanning was then reduced by 20× zooming. Complete photobleach was achieved after 60 scans at full laser power (0.2 s each). After returning the settings to initial mode, fluorescence refill was evaluated after 2 min and calculated by: $\%\text{refill} = (I_{2\ \min} - I_o)/I_o$, where I_o is pixel intensity of CDCF fluorescence emission in the target cell right after bleach and $I_{2\ \min}$ is pixel intensity in the same cell 2 min after bleaching [27].

Measurement of cell proliferation by MTT assay

Cells were seeded at a density of 1×10^4 cells/well into 96-well plates and 24-well plates, cultured for 24–36 h, and divided into different groups as described above. MTT (5 mg/ml) was added to the wells (20 μl/well) at the end of the experiment. After 4 h of incubation at 37°C, the media were removed from the wells, and DMSO was added (150 μl/well). The plates were agitated at room temperature for 30 min. Absorbance at 490 nm was measured on a spectrophotometer microplate reader (Multiskan MK3-Thermo) [28].

Immunofluorescence localization

H9c2 cells and Wnt-3a$^+$-H9c2 cells were seeded on glass coverslips (gelatinized, carbon-coated). After 24–36 h, they were treated with 18β-GA for 24 and 48 h at 37°C, respectively, washed with phosphate-buffered saline (PBS; 137 mM NaCl, 2.7 mM KCl, 4.3 mM Na_2HPO_4, and 1.4 mM KH_2PO_4, pH 7.4), and fixed for 5 min in ice-cold polyoxymethylene for 10 min. The polyclonal rabbit primary antibodies include antibodies specific for Cx43 against the C-terminus of Cx43. Coverslips with fixed cells were washed for three times with PBS for 5 min and then incubated with primary antibodies (1:200 dilution) at 37°C for 2 h. Then the cells were washed with PBS and incubated in FITC-labeled goat secondary antibodies (1:50 dilution) at 37°C for 1 h. After extensive wash with PBS for three times for 5 min, coverslips were incubated in Hoechst 33258 at 37°C for another 30 min. Then the cells were washed with PBS and coverslips were mounted onto glass slides. The specimens were examined and digital images were acquired through a Leica microscope equipped with epifluorescence [22,29].

Ca^{2+} imaging

The change of intracellular [Ca^{2+}] was monitored by measurement of fluo-3 AM fluorescence. H9c2 cells and stably transfected with Wnt-3a constructs were cultured on 20-mm glass bottom of 35 mm^2 plate glass bottom dishes for 24–36 h and loaded by incubation in medium containing 10 μM fluo-3 AM for 30 min at room temperature. Subsequently, all the experiments were performed in culture medium at room temperature. Then cells were washed in HBSS supplemented with 10 mM HEPES, pH 7.3, for 30 min. Fluorescence images were acquired using Confocal microscopy (Leica TCS SP5) with a 488-nm excitation wavelength and a 510-nm emission wavelength. Images (512 × 512 pixels) were acquired every 0.87 s. After fluo-3 resting signal was recorded, 18β-GA or Furosemide was applied [27,30], and the changes of the fluorescence after 2 min were recorded.

ATP measurement

ATP determinations were carried out using a bioluminescent ATP assay kit and a Berthold luminometer (Berthold Technologies GmbH & Co. KG). Cells were grown in 24-well tissue culture plates. Each well was half-washed with HBSS for three times and samples of the supernatant were collected immediately before and 10 min after

exposure to 5, 10, and 15 μM of 18β-GA [31]. Then ATP in samples were measured according to the instruction of the ATP Determination Kit.

Statistics

Data were expressed as the mean ± SD. Statistical significance was assessed by the two-tailed Student's *t*-test, in which $P < 0.05$ was considered significant.

Results

18β-GA significantly increased proliferation of H9c2 cells

To investigate the effects of Cx43 GJ and hemichannel on cell proliferation, we first examined the proliferation rates of H9c2 cells treated with triplet concentrations of 18β-GA. Chung *et al*. [15] proved that the effects on gap junctional channels were maximal and almost stable when treated with 5–10 μM 18β-GA, so the doses of 18β-GA we chose were 5 and 10 μM. We also examined the effects of 15 μM 18β-GA on cell proliferation and expected to observe a more obvious change. After treating cells with 5, 10, or 15 μM of 18β-GA for 24 h, a significant increase in proliferation rate of H9c2 cells was detected. The proliferation rate was quantified as shown in **Fig. 1(A)**. The proliferation rate reached 4.5, 7.7, and 3.6 folds, respectively, when compared with control.

18β-GA augmented *Cx43* mRNA and changed Cx43 location, but restrained hemichannel activity

Liang *et al*. [29] and Chung *et al*. [15] showed that accelerated Cx43 degradation induced by 18β-GA could increase Cx43 protein level, however, the effect of 18β-GA on Cx43 transcription is not clear. *Cx43* mRNA levels of H9c2 cells were examined by RT–PCR. RT–PCR analysis displayed that *Cx43* mRNA level of H9c2 cells markedly increased with the treatment of 18β-GA [**Fig. 2(A,B)**].

To examine whether the increase in proliferation level was mediated by Cx43 channels, Cx43 location in H9c2 cells was examined by immunofluorescence.

Immunofluorescence staining with rabbit antibody against Cx43 was discriminated in cells treated with concentrations of 18β-GA. The results showed that with the treatment of 5, 10, or 15 μM 18β-GA for 24 h, Cx43 staining of H9c2 cells significant increased at cell–cell contacts where GJ plaques loacted [**Fig. 3(A)**], but no obvious change were detected in cytoplasmic staining [**Fig. 3(B–D)**].

We further examined the hemichannel activity of cell bundles by EthBr uptake and observed dimmer dye uptake fluorescence in 5, 10, or 15 μM 18β-GA treated H9c2 cells [**Fig. 4(B–D)**].

Increased *Cx43* mRNA, altered Cx43 location, and enhanced hemichannel activity in Wnt-3a$^+$-H9c2 cells

Our previous report confirmed that the expression of Cx43 in Wnt-3a$^+$-H9c2 cells was significantly increased and the proliferation of Wnt-3a$^+$-H9c2 cells was changed [17]. We want to investigate if any alteration happened on GJ assemblage and hemichannel activity in Wnt-3a$^+$-H9c2 cells.

As our *Wnt-3a* gene was bound with *Myc* gene, the presence of Myc protein was determined by western blot to confirm successful transfection. As shown in **Fig. 2(C)**, Myc had been well-characterized in the medium of Wnt-3a$^+$-H9c2 cells, but not detected in H9c2 cells or in that of pcDNA3.1-H9c2 cells. RT–PCR analysis showed that mRNA level of *Cx43* markedly increased in the

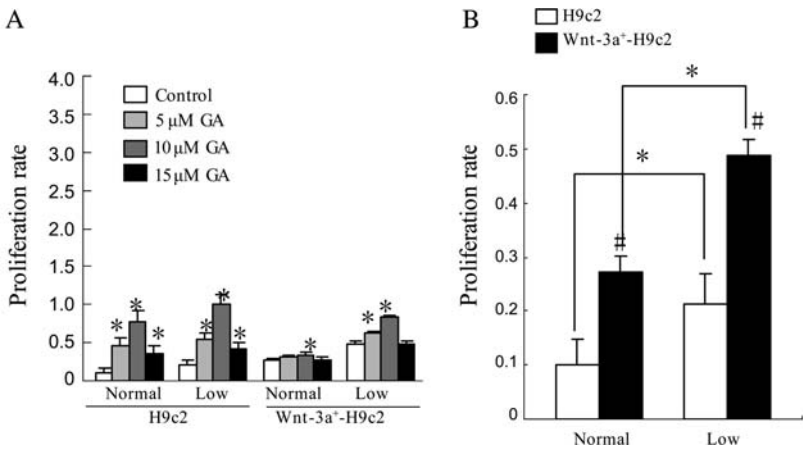

Figure 1 Effect of 18β-GA on proliferation rate of H9c2 and Wnt-3a$^+$-H9c2 cells (A) Proliferation rate in low density (Low) or normal density (Normal) cultured H9c2 cells and Wnt-3a$^+$-H9c2 cells under control conditions (control) or treated with 5, 10, or 15 μM 18β-GA (GA). Proliferation of untreated cells was assumed as 100%. Each plotted value represents the mean ± SD ($n = 6$). *$P < 0.05$ when compared with control. (B) Proliferation rate in H9c2 cells and Wnt-3a$^+$-H9c2 cells at different density. Each plotted value represents the mean ± SD ($n = 6$). *$P < 0.05$ when compared with the same kind of cells cultured at normal density and $^{\#}P < 0.05$ when compared with H9c2 cells cultured at the same density.

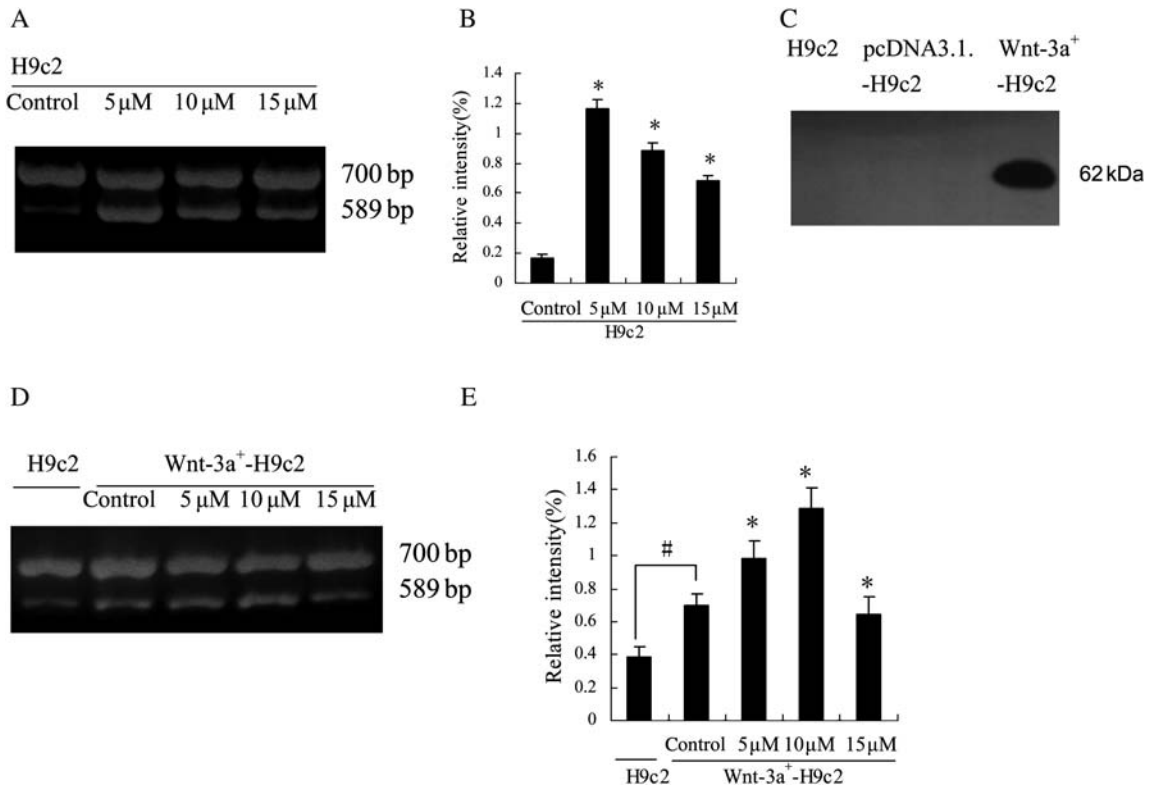

Figure 2 Western blot analysis for Myc and RT−PCR for *Cx43* in Wnt-3a$^+$-H9c2 cells (A) *Cx43* transcription in H9c2 cells with the treatment of 18β-GA as demonstrated by RT−PCR. The expression of *Cx43* (589 bp) is discernible in 18β-GA (5, 10, and 15 μM) treated cells. β-actin (700 bp) is an internal control. (B) Bars depict the effects of 18β-GA on *Cx43* transcription in H9c2 cells. Results represent the mean ± SD of three independent experiments. *$P < 0.05$ when compared with control. (C) Western blot analysis for Myc protein expression in cell medium. Myc is a secretory protein in medium and the medium were condensed by Amicon Ultra-15 Centrifugal Filter Uints. (D) *Cx43* transcription in 18β-GA treated Wnt-3a$^+$-H9c2 cells as demonstrated by RT−PCR. The expression of *Cx43* (589 bp) was discernible in 18β-GA (5, 10, or 15 μM) treated cells as demonstrated by RT−PCR. *β-actin* (700 bp) is a negative control. (E) Bars depict the effects of 18β-GA on *Cx43* transcription in Wnt-3a$^+$-H9c2 cells. Results represent the mean ± SD of three independent experiments. *$P < 0.05$ when compared with control and $^{\#}P < 0.05$ when control group of Wnt-3a$^+$-H9c2 compared with that of H9c2.

cultures of Wnt-3a$^+$-H9c2 cells and in those with the treatment of 18β-GA for 24 h [**Fig. 2(D,E)**].

The amount of Cx43 staining localization was visibly reduced in Wnt-3a$^+$-H9c2 cells at gap junctional plaques [**Fig. 3(E)**] compared with H9c2 cells whereas distinctly increased in the cytoplasm [**Fig. 3(E)**, arrows]. Treatment with 18β-GA for 24 h did not significantly enhance Cx43 staining of the GJ [**Fig. 3(F−H)**] and increased dispersed cytoplasmic staining for Cx43 [**Fig. 3(F−H)**, arrows].

Under control conditions, the amount of Wnt-3a$^+$-H9c2 cells was more than that of H9c2 cells in EthBr uptake [**Fig. 4(A,E)**]. Fewer EthBr positive cells occurred in 18β-GA (5 and 10 μM) treated Wnt-3a$^+$-H9c2 cells, and no obvious change in 15 μM 18β-GA treated cells [**Fig. 4(F−H)**].

18β-GA does not increase Wnt-3a$^+$-H9c2 proliferation

The effect of 18β-GA on proliferation of Wnt-3a$^+$-H9c2 cells was also determined. The proliferation rate in Wnt-3a$^+$-H9c2 cells was observably increased [**Fig. 1(B)**], which was consistent with our previous studies [17]. A significant increase of proliferation rate in H9c2 cells was not observed, but surprisingly, the proliferation rate of Wnt-3a$^+$-H9c2 cells was slightly increased with 10 μM 18β-GA and no significant change were observed with other concentrations [**Fig. 1(A)**].

Inhibited hemichannel activity enhances the proliferation of H9c2 and Wnt-3a$^+$-H9c2 cells

In cardiomyocytes, Wnt pathway has been considered to be involved in the regulation of proliferation [32−34] and 18β-GA is an inhibitor of GJ and hemichannel. The proliferation rate and the Cx43 transcription and intracellular location in H9c2 and Wnt-3a$^+$-H9c2 cells were not adequate to explain the alteration of the proliferation rate. As the other functions of connexins appear to be GJ- or hemichannel-independent and GJ has been indicated to be involved in cell proliferation, we supposed that Cx43 hemichannel activity may also be involved. To test the requirement of hemichannel for H9c2 cells proliferation

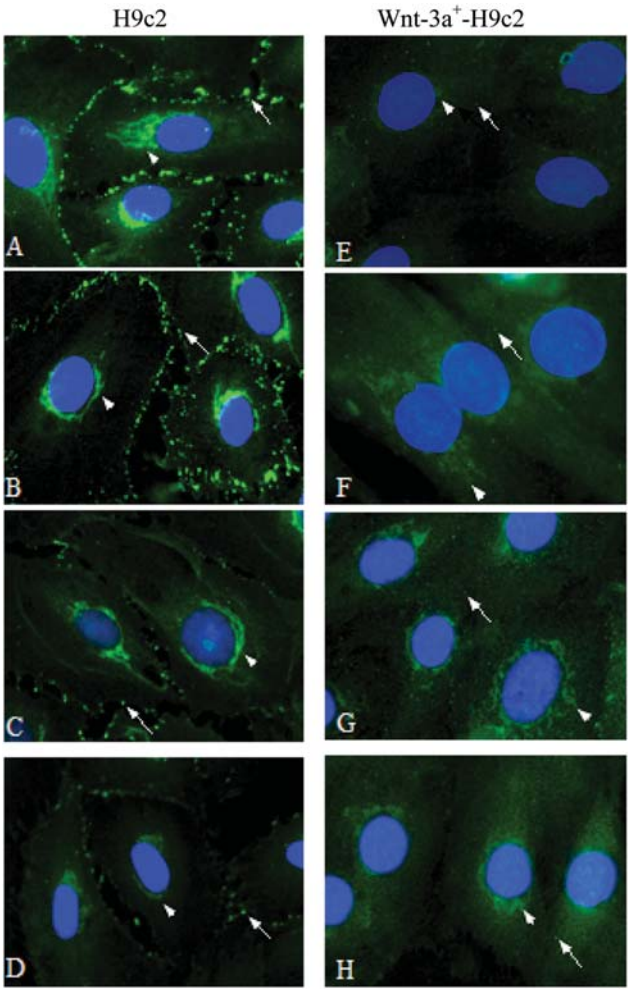

Figure 3 Immunofluorescence staining of H9c2 and Wnt-3a$^+$-H9c2 cells showing 18β-GA-induced changes of Cx43 location Cells without any treatment (A, E) or with the treatment of 5 μM (B, F), 10 μM (C, G), or 15 μM (D, H) 18β-GA for 24 h. Antibody recognizing Cx43 (green). Nuclei were stained with Hoechst 33342 (blue). The arrows in the left panels indicate the cytoplasmic distribution of total Cx43/GJ junction, and those in the right panels indicate the cytoplasmic staining for Cx43. The arrowheads indicate the distribution of total Cx43 of area surround cell nucleus.

accurately, we need to find a way to study hemichannel separately. Cells lost joint when cultured in low density whereas two hemichannels constitute GJ only when they were contributed by adjacent cells, so that GJ coupling was suppressed in cultures at low-density [24]. To analyze the regulation of hemichannel in H9c2 cells proliferation, cells were prepared at low density to ensure that the majority of the cells were not physically in contact. To demonstrate this assumption, GJ permeability was quantified in H9c2 cells at normal density or low density by FRAP. Functional gap junctional plaques in low-density cultures were primarily absent, which was consistent with our assumption (**Fig. 5**).

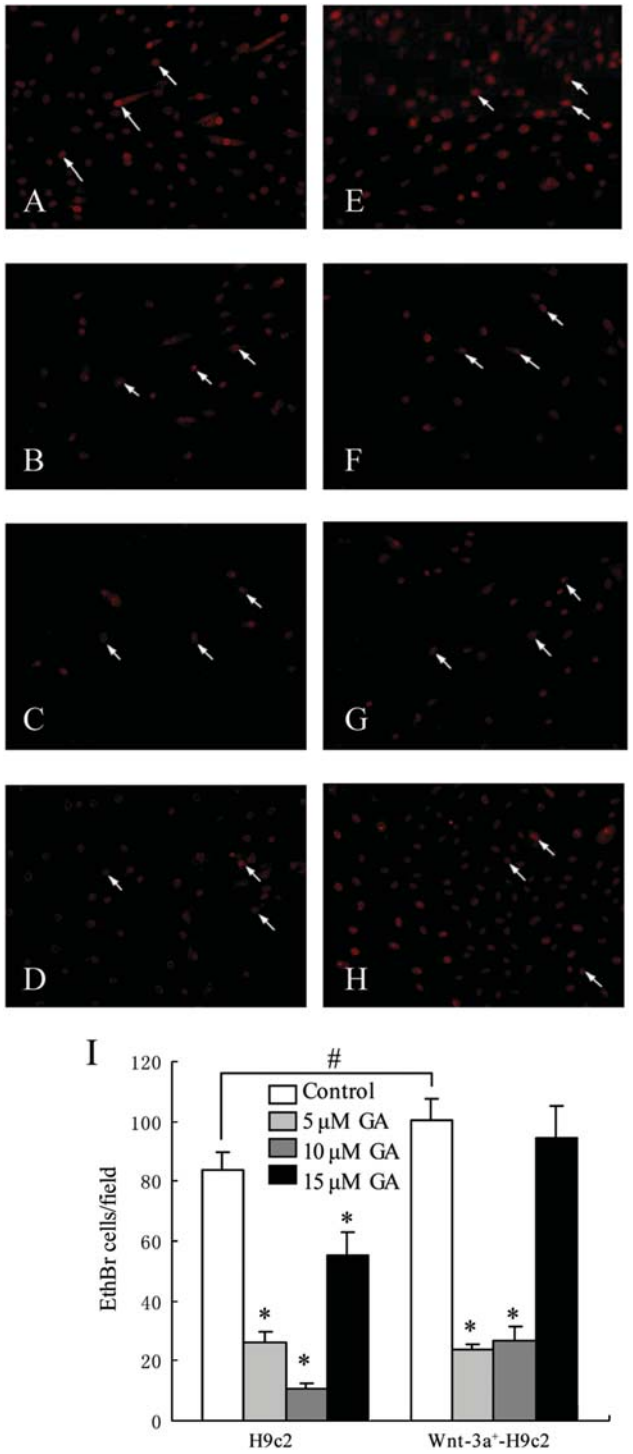

Figure 4 Addition of 18β-GA affects membrane permeability (indicate hemichannel activity) in H9c2 cells and Wnt-3a$^+$-H9c2 cells Representative pictures of EthBr uptake either in enriched H9c2 cultures (A–D) or in Wnt-3a$^+$-H9c2 cultures (E–H). Both culture models were treated with 5 μM (B, F), 10 μM (C, G), or 15 μM (D, H) 18β-GA (GA) for 10 min when the fluorescence is almost constant. The arrows indicate active cells. Each plotted number corresponds to the mean ± SD of four to six independent experiments. $^*P < 0.05$, when compared with control group and $^{\#}P < 0.05$, when control group of Wnt-3a$^+$-H9c2 cells compared with that of H9c2 cells.

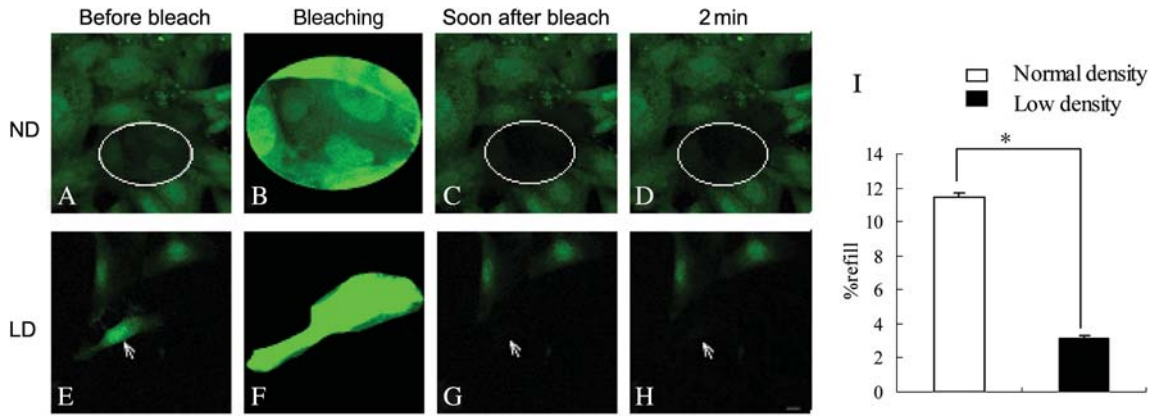

Figure 5 6-CDCF permeability decreased in low-density cultured cells (A–D) and (E–H) is H9c2 cells cultured in low density (10^3 cells/cm^2) and normal density (10^5 cells/cm^2), respectively. Then cultures were loaded with 6-CDCF (green). 6-CDCF is small molecular weight substance which can get across GJ junctions freely so that GJ junction permeability can be evaluated by fluorescence recovery after photobleach (FRAP). (A, E) 6-CDCF fluorescence before photobleach, and all cells were 6-CDCF-positive (green). The target area of photobleach is indicated by white ellipse or arrows. (B, F) 6-CDCF fluorescence in photobleach. (C, G) 6-CDCF fluorescence immediately after photobleach. (D, H) 6-CDCF fluorescence of 2 min after photobleach. (D) The cells had partly regained fluorescence because of influx of 6-CDCF from surrounding GJ junction-coupled cells in 2 min. (H) 6-CDCF fluorescence recovery significantly decreased in cultures of low density suggest inhibited GJ junction coupling. (I) Percentage of refill as a function of GJ junction. About 11.43% recovery of fluorescence occurred in cultures of normal density and 3.16% recovery in low density within 2 min. Scale bar = 10 μm. Values are presented as the mean ± SD ($n = 3$). *$P < 0.05$, compared with normal density cultures.

We compared the proliferation rate of cultures at the two densities and found that the rate increased in low-density cultured cells as shown in **Fig. 1(B)**. Then, the proliferation rates of cultures at low-density treated with drug were evaluated [**Fig. 1(A)**]. Twenty-four hours of incubation with 18β-GA of different concentrations (5, 10, and 15 μM) also caused phenotypic increase of cell proliferation in H9c2 cells (2.6, 4.7, and 2.0 folds compared with control, respectively) at low-density, similar to those observed in the presence of drug in a group of cells at normal density. The increase fold of 1.3, 1.7, and 1.0, respectively, was still elevated in Wnt-3a$^+$-H9c2 cells.

Inhibited hemichannel enhanced H9c2 cells intracellular [Ca^{2+}]

To elucidate the mechanism by which the inhibited hemichannels influences the proliferation of H9c2 cells, the change of intracellular calcium of the cells with the treatment of 18β-GA was examined. Because the prominent inhibition of hemichannel activity and enhancement of proliferation rate was observed when H9c2 cells were treated with 10 μM 18β-GA, [Ca^{2+}] of H9c2, and Wnt-3a$^+$-H9c2 cells loaded with fluo-3 AM [35] was monitored in 2 min when the fluorescence was in balance. As shown in **Fig. 6(A,E)**, the intracellular [Ca^{2+}] decreased rapidly in H9c2 cells incubated without drug because of fluorescence quenching effect. In 10 μM 18β-GA treated cultures, the suppression of [Ca^{2+}] was fairly reversed [**Fig. 6(B,F)**]. This trend was also observed in Wnt-3a$^+$-H9c2 cells [**Fig. 6(C,G,D,H)**].

Increased intracellular [Ca^{2+}] was not mediated by ATP alteration induced by inhibited hemichannel

In order to investigate the ATP requirement for calcium signaling, the ATP concentration in cultures treated with 10 μM 18β-GA was detected [**Fig. 7(A)**]. The data showed that with the treatment of 18β-GA, the amount of intracellular ATP in H9c2 cells significantly increased, but in Wnt-3a$^+$-H9c2 cells, it is decreased.

Discussion

Cx43 has been shown to be a downstream target of Wnt pathway and Wnt/β-catenin signaling pathway in many cell types, including ovarian endometrioid adenocarcinomas (OEAs) and osteoblasts [36–38]. In mammary epithelial cells, Wnt-3a has been shown to up-regulate the expression of *Cx43* gene and phenotypically increased transepithelial resistance across the cell monolayer [39]. Zhai *et al.* [37] showed differences in the expression of *Cx43* transcripts in OEAs with β-catenin defects versus OEAs with intact β-catenin regulation, which highlights the potential role of β-catenin in the regulation of *Cx43* gene expression. Consistent with these previous studies, our study showed that Wnt-3a$^+$-H9c2 cells enhanced transcription of *Cx43* mRNA [**Fig. 2(B,D)**]. Liang *et al.* [29] and Chung *et al.* [15] showed that accelerated *Cx43* degradation induced by 18β-GA [15] could increase Cx43 protein level. In our experiment, H9c2 and Wnt-3a$^+$-H9c2 cells treated with 18β-GA increased *Cx43* transcription level [**Fig. 2(B–E)**], which may be a response to inhibit cell permeability [15]. Ai *et al.* [40] found

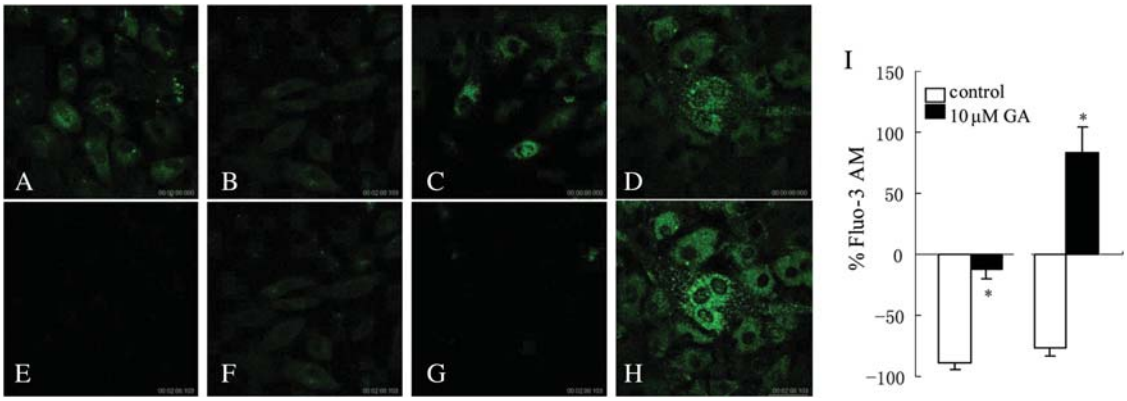

Figure 6 Intracellular [Ca^{2+}] of H9c2 and Wnt-3a^{+}-H9c2 cells treated with 10 μM 18β-GA Free [Ca^{2+}] was marked by calcium indicators, flou3-AM, and showed green. H9c2 cells without any treatment (A, E) or treated with 10 μM (B, F) 18β-GA for 2 min, when the fluorescence in balance. Wnt-3a^{+}-H9c2 cells without any treatment (C, G), or treated with 10 μM (D, H) 18β-GA (GA) for 2 min. (I) Mean ± SD ($n = 3$) percentage of calcium fluorescence under control conditions (white bar), or with 10 μM 18β-GA present in the culture media (black bar). Scale bar = 50 μm. *$P <$ 0.05 when compared with control.

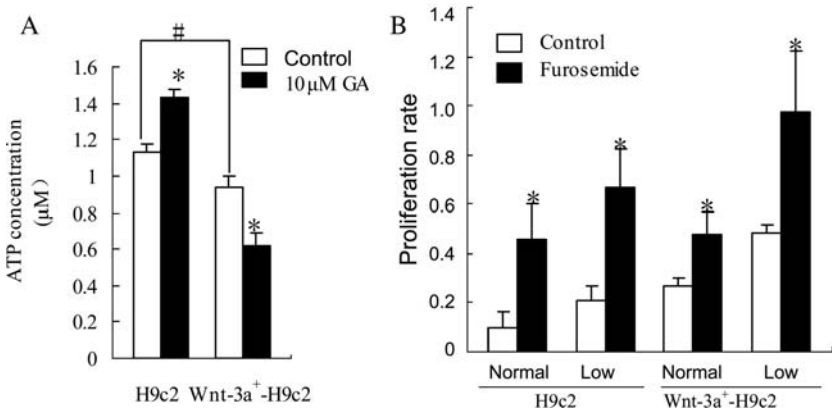

Figure 7 Intracellular ATP and effect of furosemide on proliferation of H9c2 and Wnt-3a^{+}-H9c2 cells (A) Changes of intracellular ATP concentration in H9c2 cells and Wnt-3a^{+}-H9c2 cells in the presence of 10 μM 18β-GA (GA). Data represent the mean ± SD of three separated experiments. *$P < 0.05$ when compared with control and $^{\#}P < 0.05$ when control group of Wnt-3a^{+}-H9c2 cells compared with that of H9c2 cells. (B) Proliferation rate in low density or normal density cultured H9c2 cells and Wnt-3a^{+}-H9c2 cells under control conditions (control) or treated with 5 μM furosemide. Results represent the mean ± SD of three independent experiments. *$P < 0.05$ when compared with control.

that Cx43 expression was induced by secrete bioactive Wnt-1 in cardiomyocytes and cardiomyocyte Lucifer yellow dye transfer was enhanced, but hemichannel activity was not examined. We found that hemichannel activity was also increased in Wnt-3a^{+}-H9c2 cells as determined by EthBr dye uptake [**Fig. 4(A,E,I)**]. The nearly balanced proliferation rate of Wnt-3a^{+}-H9c2 cells with the treatment of 18β-GA may indicate that the enhanced activity of hemichannel induced by *Wnt-3a* exactly counteract with the negative effect of 18β-GA on hemichannel and cut the positive effect of the latter on the proliferation [**Fig. 1(A)**]. Whereas, Wnt proteins prevent apoptosis of both uncommitted osteoblast progenitors and differentiated osteoblasts by β-catenin-dependent and -independent signaling cascades involving Src/ERK and phosphatidylinositol 3-kinase/AKT [41]. Wnt-3a induce LRP5-independent transient phosphorylation of ERKs, Src, and Akt, and prolong the survival of osteoblasts and osteoblast progenitors. Furthermore, Src can affect Cx43 activity by directly phosphorylating Cx43 at tyrosine residues or recruiting kinases, such as MAPK (mitogen activated protein kinase), PKC (protein kinase C) or by other mechanisms to phosphorylate Cx43 to block gap junctional communication [42]. So *Wnt-3a* may phosphorylate Cx43 and induce inhibition of gap junctional communication. Also in our study, diminution of the amount of Cx43 GJ plaques was observed in Wnt-3a^{+}-H9c2 cells [**Fig. 3(E−H)**]. Therefore, the effects of Wnt-3a on Cx43 GJ need to be further studied. The hemichannel activities of Wnt-3a^{+}-H9c2 with the treatment of 5 and 10 μM 18β-GA were almost same [**Fig. 4(F,G,I)**]. This is because the effects of many signaling pathways, including what we mentioned above, on hemichannel activity was nearly in balance under those conditions.

Previous studies demonstrated that granulosa cells need to express Cx43 to maintain its proliferation and response to an oocyte-derived mitogen [43]. Inhibition of Cx37 displayed a lower proliferation rate, whereas knockdown of Cx43 will not. This indicates a major role for Cx37 mediated communication with granulosa cells during mouse oocytes development [44]. Li *et al*. [45] observed decreased speed of cell locomotion and cell proliferation rate in the Cx43-deficient proepicardial cells and showed an important role for Cx43 in human cardiovascular anomalies. In our research, the amount of *Cx43* transcription was increased with the treatment of 5–10 μM 18β-GA [**Fig. 2(B–E)**]; however, the changes of proliferation with the same treatment displayed different increase trends [**Fig. 1(A)**], which hinted that there must be other mechanisms involved in the effect of Cx43 on H9c2 cell proliferation. Cytoplasm Cx43 significantly increased in Wnt-3a$^+$-H9c2 cells with the treatment of 18β-GA, as determined by immunofluorescence staining [**Fig. 3(F–H)**], which may be one of the factors for the change of Wnt-3a$^+$-H9c2 cell proliferation, as carboxyl terminus of Cx43 can possibly interact with other proteins localized in the cytoplasm or nucleus to exhibit cell growth suppression function [46,47]. Furthermore, GJs were suggested to be involved in cell growth suppression [48–50], so cells cultured at low density to block GJ induced increase in both H9c2 and Wnt-3a$^+$-H9c2 cell proliferation [**Fig. 1(B)**]. Gap junction-independent pathway may contributed much more than the GJ-dependent one on the Cx43-induced cell growth suppression by targeting the proto-oncogene SKP2 and consequently increasing the level of the cell cycle controller p27 [8]. Therefore, in our experiments, increased cytoplasm Cx43 induced cell growth suppression may counteract the effects of inhibited GJ induced cell growth promotion in Wnt-3a$^+$-H9c2 cells treated with 18β-GA [**Fig. 1(A)**].

Lucifer yellow dye coupling showed the inhibited effects of 5–10 μM 18β-GA on gap junctional channels were maximal and almost stable. In our study, however, the proliferation rates of cells treated with different concentrations of 18β-GA were enhanced in different manners. So hemichannel may be involved in regulation of cell proliferation. Further study proved the hypothesis, the examination of cell proliferation rate and hemichannel activity with the treatment of 5 and 10 μM 18β-GA showed that when hemichannel activity was inhibited, cell proliferation rate increased and these changes were dose-dependent. We also used 15 μM 18β-GA and observed that it seemed to cause nonspecific increase in cell proliferation in H9c2 cells. Studies in low density also confirmed it. Cells were cultured in low density to block GJ, and treated with 18β-GA. Significant increase of proliferation rates were observed at the dose of 5 and 10 μM [**Fig. 1(A)**]. About 15 μM 18β-GA also seemed to cause a nonspecific increase in cell proliferation. These results suggested that hemichannel are largely involved in the regulation of H9c2 cell proliferation. Cultures in low-density displayed higher proliferation rate may also confirm that GJ contribute to the maintenance of normal cell proliferation [8].

Release of ATP through the spontaneous gating of connexin hemichannels in cells of the RPE induced intracellular [Ca^{2+}] release from the radial Glia [51]. In H9c2 cells, inhibited hemichannels decreased ATP release and increased intracellular ATP, whereas stimulated hemichannel activity mediated by Wnt-3a decreased intracellular ATP [**Fig. 7(A)**]. In chick retinal explants, ATP and ADP induce the accumulation of [^{3}H]-phosphoinositides and a transient activation of the ERK pathway, which lead to represent of phospho-ERK and BrdU labeled cells and mediate the effect on DNA synthesis [52]. ATP, as a neurotransmitter, can induce transient Ca^{2+} signaling. It acts on purinergic receptors and has been proposed to promote proliferation and accelerate DNA synthesis in neural retinal progenitor cells [20]. Within early stages of the development of the neural chick retina, the release of ATP through GJ Cx43 hemichannels from RPE acts on progenitor cells to speed cell division or evoke Ca^{2+} transients and to speed their mitosis [20,53,54]. Thus, increased intracellular ATP may lead to [Ca^{2+}] and proliferation rate increased in Wnt-3a$^+$-H9c2 cells [**Fig. 6(C,G,I)**]. To block connexin hemichannel but not GJ channels would inhibit the propagation of Ca^{2+} responses to cells adhesion [55]. The initiation of Ca^{2+} waves evoked by hemichannel activation may control cell cycle events during early prenatal neurogenesis [56]. Ca^{2+} signaling induced by cADPR generated from NAD^+ released through Cx43 hemichannels increase the proliferation rate in 3T3 fibroblasts via shorten its S phase [11]. In vascular smooth muscle cells, calcium channel blocker, enidipine, inhibited cell cycle progression, and presence anti-proliferative actions via the expression of smooth muscle myosin heavy chain (SM2) [57]. Intracellular [Ca^{2+}] increased in H9c2 cells were induced by hemichannel blockade [**Fig. 6(A,B,E,F,I)**] and resulted in promotion of cell proliferation. These results suggested that connexins played a dual pivotal role in Ca^{2+} signaling and proliferation in H9c2 cells: inhibited hemichannel may represent a key step in restraining ATP release, which lead to propagation of Ca^{2+} spreading restriction and cell proliferation depression; whereas, hindered diffusion of Ca^{2+} through GJ channels decreased activation of second messengers across adjacent cells and increased cell proliferation.

A group of genes controlling ATP release were identified downstream of Wnt/β-catenin pathway, so that decrease of ATP in Wnt-3a$^+$-H9c2 cells [**Fig. 7(A)**] with the treatment of 18β-GA may be induced by other pathways.

Intracellular ATP could be regulated by Cl^- channels (connexins regulate calcium signaling by controlling ATP release), so we supposed that ATP efflux via activated Cl^- channels which is independent from hemichannels and induced increased proliferation of Wnt-3a$^+$-H9c2 cells. However, inhibited Cl^- channels by Furosemide showed no increased rates of proliferation of Wnt-3a$^+$-H9c2 cells compared with H9c2 cells [**Fig. 7(B)**]. Wnt-1 stimulates 3T3-L1 preadipocytes to secrete factors, including insulin-like growth factor I (IGF-I) and IGF-II, that increase PKB/Akt phosphorylation and allow these cells to survive in serum deprivation [58]. IP3 receptor (IP3R) is an *in vivo* substrate for Akt kinase and IP3Rs can be phosphorylated by Akt kinase *in vitro* and *in vivo* [59]. The IP3-dependent ATP release is involved in astrocytic cells, that is ATP release through an IP3-protein-dependent pathway mediates intercellular calcium signaling [60]. So this pathway may exist in the regulation of intracellular ATP-mediated by Wnt-3a, which needs further study.

In conclusion, our results indicated that hemichannel was involved in regulation of H9c2 cell proliferation. Enhanced proliferation was induced by increased intracellular ATP and [Ca^{2+}], which was caused by inhibited hemichannel. This study also showed a complex network, including proteins, small molecular materials, and signal pathways, in the modulation of cell proliferation. Our future work will focus on the mechanism of modulation of intracellular ATP-mediated by Wnt-3a as we mentioned above.

References

1 Söhl G and Willecke K. An update on connexin genes and their nomenclature in mouse and man. Cell Commun Adhes 2003, 10: 173–180.

2 Essenfelder GM, Bruzzone R, Lamartine J, Charollais A, Blanchet-Bardon C, Barbe MT, Meda P and Waksman G. Connexin 30 mutations responsible for hidrotic ectodermal dysplasia cause abnormal hemichannel activity. Hum Mol Genet 2004, 13: 1703–1714.

3 George CH, Kendall JM and Evans WH. Intracellular trafficking pathways in the assembly of connexins into gap junctions. J Biol Chem 1999, 274: 8678–8685.

4 Sarma JD, Wang F and Koval M. Targeted gap junction protein constructs reveal connexin-specific differences in oligomerization. J Biol Chem 2002, 277: 20911–20918.

5 Ramachandran S, Xie LH, John SA, Subramaniam S and Lal R. A novel role for connexin hemichannel in oxidative stress and smoking-induced cell injury. PLoS One 2007, 2: e712.

6 Lauf U, Giepmans BN, Lopez P, Braconnot S, Chen SC and Falk MM. Dynamic trafficking and delivery of connexons to the plasma membrane and accretion to gap junctions in living cells. Proc Natl Acad Sci USA 2002, 99: 10446–10451.

7 King TJ and Bertram JS. Connexins as targets for cancer chemoprevention and chemotherapy. Biochim Biophys Acta 2005, 1719: 146–60.

8 Jiang JX and Gu S. Gap junction- and hemichannel-independent actions of connexins. Biochim Biophys Acta 2005, 1711: 208–14.

9 Quist AP, Rhee SK, Lin H and Lal R. Physiological role of gap-junctional hemichannels: extracellular calcium-dependent isosmotic volume regulation. J Cell Biol 2000, 148: 1063–1074.

10 Bruzzone S, Guida L, Zocchi E, Franco L and De Flora A. Connexin 43 hemi channels mediate Ca^{2+} regulated transmembrane NAD+ fluxes in intact cells. FASEB J 2001, 15: 10–12.

11 Franco L, Zocchi E, Usai C, Guida L, Bruzzone S, Costa A and De Flora A. Paracrine roles of NAD^+ and cyclic ADP-ribose in increasing intracellular calcium and enhancing cell proliferation of 3T3 fibroblasts. J Biol Chem 2001, 276: 21642–21648.

12 Stout CE, Costantin JL, Naus CC and Charles AC. Intercellular calcium signaling in astrocytes via ATP release through connexin hemichannels. J Biol Chem 2002, 277: 10482–10488.

13 Davidson JS and Baumgarten IM. Glycyrrhetinic acid derivatives: a novel class of inhibitors of gap-junctional intercellular communication. Structure-activity relationships. J Pharmacol Exp Ther 1988, 246: 1104–1107.

14 Contreras JE, Sánchez HA, Eugenin EA, Speidel D, Theis M, Willecke K, Bukauskas FF and Bennett MV, *et al*. Metabolic inhibition induces opening of unapposed connexin 43 gap junction hemichannels and reduces gap junctional communication in cortical astrocytes in culture. Proc Natl Acad Sci USA 2002, 99: 495–500.

15 Chung TH, Wang SM, Chang YC, Chen YL and Wu JC. 18beta-glycyrrhetinic acid promotes Src interaction with Connexin 43 in rat cardiomyocytes. J Cell Biochem 2007, 100: 653–664.

16 Meyer RA, Cohen MF, Recalde S, Zakany J, Bell SM, Scott WJ, Jr and Lo CW. Developmental regulation and asymmetric expression of the gene encoding Cx43 gap junctions in the mouse limb bud. Dev Genet 1997, 21: 290–300.

17 Liu X, Liu W, Yang L, Xia B, Li J, Zuo J and Li X. Increased connexin 43 expression improves the migratory and proliferative ability of H9c2 cells by Wnt-3a overexpression. Acta Biochim Biophys Sin 2007, 39: 391–398.

18 Kunapuli SP and Daniel JL. P2 receptor subtypes in the cardiovascular system. Biochem J 1998, 336: 513–523.

19 Sanches G, de Alencar LS and Ventura AL. ATP induces proliferation of retinal cells in culture via activation of PKC and extracellular signal-regulated kinase cascade. Int J Dev Neurosci 2002, 20: 21–27.

20 Pearson RA, Dale N, Llaudet E and Mobbs P. ATP released via gap junction hemichannels from the pigment epithelium regulates neural retinal progenitor proliferation. Neuron 2005, 46: 731–744.

21 Koizumi S, Fujishita K and Inoue K. Regulation of cell-to-cell communication mediated by astrocytic ATP in the CNS. Purinergic Signal 2005, 1: 211–217.

22 Dong L, Liu X, Li H, Vertel BM and Ebihara L. Role of the N-terminus in permeability of chicken connexin45.6 gap junctional channels. J Physiol 2006, 576: 787–799.

23 Decrock E, De Vuyst E, Vinken M, Van Moorhem M, Vranckx K, Wang N and Van Laeken L, *et al*. Connexin 43 hemichannels contribute to the propagation of apoptotic cell death in a rat C6 glioma cell model. Cell Death Differ 2009, 16: 151–163.

24 Boengler K, Konietzka I, Buechert A, Heinen Y, Garcia-Dorado D, Heusch G and Schulz R. Loss of ischemic preconditioning's cardioprotection in aged mouse hearts is associated with reduced gap junctional and mitochondrial levels of connexin 43. Am J Physiol Heart Circ Physiol 2007, 292: H1764–H1769.

25 Retamal MA, Froger N, Palacios-Prado N, Ezan P, Sáez PJ, Sáez JC and Giaume C. Cx43 hemichannels and gap junction channels in astrocytes are regulated oppositely by proinflammatory cytokines released from activated microglia. J Neurosci 2007, 27: 13781–13792.

26 Riddle RC, Taylor AF, Rogers JR and Donahue HJ. ATP release mediates fluid flow-induced proliferation of human bone marrow stromal cells. J Bone Miner Res 2007, 22: 589–600.

27 Giles WR and Smith GL. Evidence of intercellular coupling between co-cultured adult rabbit ventricular myocytes and myofibroblasts. J Physiol 2007, 583: 225–236.
28 Wang T, Zhang ZX, Xu YJ and Hu QH. 5-Hydroxydecanoate inhibits proliferation of hypoxic human pulmonary artery smooth muscle cells by blocking mitochondrial K (ATP) channels. Acta Pharmacol Sin 2007, 28: 1531–1540.
29 Liang JY, Wang SM, Chung TH, Yang SH and Wu JC. Effects of 18-glycyrrhetinic acid on serine 368 phosphorylation of Connexin 43 in rat neonatal cardiomyocytes. Cell Biol Int 2008, 32: 1371–1379.
30 Zhu CH, Lu FP, He YN, Han ZL and Du LX. Regulation of avilamycin biosynthesis in Streptomyces viridochromogenes: effects of glucose, ammonium ion, and inorganic phosphate. Appl Microbiol Biotechnol 2007, 73: 1031–1038.
31 Formigli L, Francini F, Tani A, Squecco R, Nosi D, Polidori L and Nistri S, *et al*. Morphofunctional integration between skeletal myoblasts and adult cardiomyocytes in coculture is favored by direct cell-cell contacts and relaxin treatment. Am J Physiol Cell Physiol 2005, 288: C795–804.
32 Kim SE and Choi KY. EGF receptor is involved in WNT3a-mediated proliferation and motility of NIH3T3 cells via ERK pathway activation. Cell Signal 2007, 19: 1554–64.
33 Kim SE, Lee WJ and Choi KY. The PI3 kinase-Akt pathway mediates Wnt3a-induced proliferation. Cell Signal 2007, 19: 511–518.
34 Jia L, Zhou J, Peng S, Li J, Cao Y and Duan E. Effects of Wnt3a on proliferation and differentiation of human epidermal stem cells. Biochem Biophys Res Commun 2008, 368: 483–488.
35 Loughrey CM, MacEachern KE, Cooper J and Smith GL. Measurement of the dissociation constant of Fluo-3 for Ca^{2+} in isolated rabbit cardiomyocytes using Ca^{2+} wave characteristics. Cell Calcium 2003, 34: 1–9.
36 Du WJ, Li JK, Wang QY, Hou JB and Yu B. Lithium chloride regulates Connexin 43 in skeletal myoblasts in vitro: possible involvement in Wnt/beta-catenin signaling. Cell Commun Adhes 2008, 15: 261–271.
37 Zhai Y, Wu R, Schwartz DR, Darrah D, Reed H, Kolligs FT and Nieman MT, *et al*. Role of beta-catenin/T-cell factor-regulated genes in ovarian endometrioid adenocarcinomas. Am J Pathol 2002, 160: 1229–1238.
38 Robinson JA, Chatterjee-Kishore M, Yaworsky PJ, Cullen DM, Zhao W, Li C and Kharode Y, *et al*. Wnt/β-catenin signaling is a normal physiological response to mechanical loading in bone. J Biol Chem 2006, 281: 31720–31728.
39 Constantinou T, Baumann F, Lacher MD, Saurer S, Friis R and Dharmarajan A. SFRP-4 abrogates Wnt-3a-induced beta-catenin and Akt/PKB signaling and reverses a Wnt-3a-imposed inhibition of in vitro mammary differentiation. J Mol Signal 2008, 3: 10.
40 Ai Z, Fischer A, Spray DC, Brown AM and Fishman GI. Wnt-1 regulation of Connexin 43 in cardiac myocytes. J Clin Invest 2000, 105: 161–171.
41 Almeida M, Han L, Bellido T, Manolagas SC and Kousteni S. Wnt proteins prevent apoptosis of both uncommitted osteoblast progenitors and differentiated osteoblasts by beta-catenin-dependent and -independent signaling cascades involving Src/ERK and phosphatidylinositol 3-kinase/AKT. J Biol Chem 2005, 280: 41342–41351.
42 Pahujaa M, Anikin M and Goldberg GS. Phosphorylation of connexin43 induced by Src: regulation of gap junctional communication between transformed cells. Exp Cell Res 2007, 313: 4083–4090.
43 Tong D, Li TY, Naus KE, Bai D and Kidder GM. In vivo analysis of undocked connexin 43 gap junction hemichannels in ovarian granulosa cells. J Cell Sci 2007, 120: 4016–4024.
44 Gittens JE and Kidder GM. Differential contributions of connexin37 and Connexin 43 to oogenesis revealed in chimeric reaggregated mouse ovaries. J Cell Sci 2005, 118: 5071–5078.
45 Li WE, Waldo K, Linask KL, Chen T, Wessels A, Parmacek MS, Kirby ML and Lo CW. An essential role for connexin 43 gap junctions in mouse coronary artery development. Development 2002, 129: 2031–42.
46 Moorby C and Patel M. Dual functions for connexins: Cx43 regulates growth independently of gap junction formation. Exp Cell Res 2001, 271: 238–248.
47 Dang XT, Doble BW and Kardami E. The carboxy-tail of connexin-43 localizes to the nucleus and inhibits cell growth. Mol Cell Biochem 2003, 242: 35–38.
48 Yamasaki H, Krutovskikh V, Mesnil M, Tanaka T, Zaidan-Dagli ML and Omori Y. Role of connexin (gap junction) genes in cell growth control and carcinogenesis. C R Acad Sci III 1999, 322: 151–159.
49 Mesnil M. Connexins and cancer. Biol Cell 2002, 94: 493–500.
50 Yamasaki H and Naus CCG. Role of connexin genes in growth control. Carcinogenesis 1996, 17: 1199–1213.
51 Dale N. Dynamic ATP signaling and neural development. J Physiol 2008, 586: 2429–2436.
52 Nunes PH, Calaza Kda C, Albuquerque LM, Fragel-Madeira L, Sholl-Franco A and Ventura AL. Signal transduction pathways associated with ATP-induced proliferation of cell progenitors in the intact embryonic retina. Int J Dev Neurosci 2007, 25: 499–508.
53 Pearson R, Catsicas M, Becker D and Mobbs P. Purinergic and muscarinic modulation of the cell cycle and calcium signaling in the chick retinal ventricular zone. J Neurosci 2002, 22: 7569–7579.
54 Webb SE and Miller AL. Calcium signaling during embryonic development. Nat Rev Mol Cell Biol 2003, 4: 539–551.
55 Anselmi F, Hernandez VH, Crispino G, Seydel A, Ortolano S, Roper SD and Kessaris N,, *et al*. . ATP release through connexin hemichannels and gap junction transfer of second messengers propagate Ca^{2+} signals across the inner ear. Proc Natl Acad Sci USA 2008, 105: 18770–18775.
56 Bruzzone R and Dermietzel R. Structure and function of gap junctions in the developing brain. Cell Tissue Res 2006, 326: 239–248.
57 Arakawa E and Hasegawa K. Benidipine, a calcium channel blocker, regulates proliferation and phenotype of vascular smooth muscle cells. J Pharmacol Sci 2006, 100: 149–156.
58 Longo KA, Kennell JA, Ochocinska MJ, Ross SE, Wright WS and MacDougald OA. Wnt signaling protects 3T3-L1 preadipocytes from apoptosis through induction of insulin-like growth factors. J Biol Chem, 2002, 277: 38239–38244.
59 Khan MT, Wagner L, Yule DI, Bhanumathy C and Joseph SK. Akt kinase phosphorylation of inositol 1,4,5-trisphosphate receptors. J Biol Chem 2006, 281: 3731–3737.
60 Stamatakis M and Mantzaris NV. Modeling of ATP-mediated signal transduction and wave propagation in astrocytic cellular networks. J Theor Biol 2006, 241: 649–668.